Preprint typeset in JHEP style - HYPER VERSION

Thermal leptogenesis and the gravitino problem in the Asaka-Yanagida axion/axino dark matter scenario

Howard Baer[a], **Sabine Kraml**[b], **Andre Lessa**[a] **and Sezen Sekmen**[c]

[a] *Dept. of Physics and Astronomy, University of Oklahoma, Norman, OK 73019, USA*
[b] *Laboratoire de Physique Subatomique et de Cosmologie, UJF Grenoble 1, CNRS/IN2P3, INPG, 53 Avenue des Martyrs, F-38026 Grenoble, France*
[c] *Dept. of Physics, Florida State University, Tallahassee, FL 32306, USA*
E-mail: baer@nhn.ou.edu, sabine.kraml@lpsc.in2p3.fr, lessa.a.p@gmail.com, sezen.sekmen@cern.ch

Abstract: A successful implementation of thermal leptogenesis requires the re-heat temperature after inflation T_R to exceed $\sim 2\times 10^9$ GeV. Such a high T_R value typically leads to an overproduction of gravitinos in the early universe, which will cause conflicts, mainly with BBN constraints. Asaka and Yanagida (AY) have proposed that these two issues can be reconciled in the context of the Peccei-Quinn augmented MSSM (PQMSSM) if one adopts a mass hierarchy $m(\text{sparticle}) > m(\text{gravitino}) > m(\text{axino})$, with $m(\text{axino}) \sim$ keV. In this case, sparticle decays bypass the gravitino, and decay more quickly to the axino LSP, thus avoiding the BBN constraints. In addition, thermally produced gravitinos decay inertly to axion+axino, also avoiding BBN constraints. We calculate the relic abundance of mixed axion/axino dark matter in the AY scenario, and investigate under what conditions a value of T_R sufficient for thermal leptogenesis can be generated. A high value of PQ breaking scale f_a is needed to suppress overproduction of axinos, while a small vacuum misalignment angle θ_i is needed to suppress overproduction of axions. The large value of f_a results in late decaying neutralinos. We show that, to avoid BBN constraints, the AY scenario requires a rather low thermal abundance of neutralinos, while higher values of neutralino mass also help. We combine these constraint calculations along with entropy production from late decaying saxions, and find the saxion needs to be typically at least several times heavier than the gravitino. A successful implementation of the AY scenario suggests that LHC should discover a spectrum of SUSY particles consistent with weak scale supergravity; that the apparent neutralino abundance is low; that a possible axion detection signal (probably with m_a in the sub-μeV range) exists, but no direct or indirect signals for WIMP dark matter should be observed.

Keywords: Supersymmetry Phenomenology, Supersymmetric Standard Model, Dark Matter.

1. Introduction

A wide assortment of data from atmospheric, solar, reactor and accelerator experiments can all be explained in terms of massive neutrinos with large mixing angles which undergo flavor oscillations upon propagation through matter or the vacuum [1]. The emerging picture of the physics behind neutrino oscillation data is most elegantly explained by the presence of massive gauge singlet right-hand Majorana neutrino states N_i ($i = 1 - 3$ a generation index) which give rise to see-saw neutrino masses [2]: $m_{\nu_i} \simeq (f_{\nu_i} v)^2/M_{N_i}$ with f_{ν_i} the neutrino Yukawa coupling, v the vev of the Higgs field, and $M_{N_i} \sim 10^9 - 10^{15}$ GeV.

In addition to explaining neutrino oscillation data, the presence of massive N_i states offers an elegant explanation of baryogenesis in terms of leptogenesis [3], wherein the states N_i exist in thermal equilibrium in the early universe, but decay asymmetrically to leptons versus anti-leptons. The lepton-anti-lepton asymmetry is then converted to a baryon asymmetry via B and L violating, but $B - L$ conserving, sphaleron effects [4]. To realize the thermal leptogenesis scenario, a re-heat temperature of the universe after inflation of $T_R \gtrsim 2 \times 10^9$ GeV is required [5].

Augmenting the Standard Model with a new, extremely high energy scale M_{N_i} naturally leads to severe quadratic divergences in the Higgs sector which will need to be highly fine-tuned. The solution here is to also incorporate supersymmetry (SUSY), which reduces quadratic divergences to merely logarithmic, and ameliorates the fine-tuning problem [6]. While the addition of weak scale softly broken SUSY into the theory is actually supported by the measured values of the gauge couplings from LEP experiments, it also leads to new conundrums such as the gravitino problem: the production of gravitinos in the early universe can lead to *(i)* overproduction of LSP dark matter (*e.g.* the lightest neutralino) beyond relic density limits obtained from WMAP and other experiments, or *(ii)* disruption of the successful explanation of Big Bang nucleosynthesis by introducing late decaying quasi-stable particles whose decay products can break up the newly minted light elements. The common solution to the gravitino problem [7] is to require a sufficiently low re-heat temperature such that thermal gravitino production is suppressed enough to avoid overproduction of dark matter or disruption of BBN [8]. For gravitino masses in the few TeV or below range, a value of $T_R \lesssim 10^5$ GeV is required. Naively, this is in obvious conflict with the T_R requirements of thermal leptogenesis.

A variety of solutions have been proposed to reconcile leptogenesis with the SUSY gravitino problem. One is to abandon the "thermal" aspect of leptogenesis, and invoke non-thermal leptogenesis wherein the heavy neutrino states are produced via some scalar field decay, for instance the inflaton [9]. Another suggestion is to invoke the gravitino as LSP, so it does not decay. However, the gravitino LSP scenarios fall back into the BBN problem since then the NLSP SUSY particle suffers a late decay into gravitino plus SM states which again injects high energy particles into the post-BBN plasma. One solution is to speed up NLSP decay via a small component of R-parity violation [10, 11].

In a recent work [12], we proposed an alternative scenario, invoking mixed axion/axino dark matter, as would occur in the Peccei-Quinn [13–16] augmented MSSM (the PQMSSM) [17, 18]. In this case, we invoked models with very heavy gravitinos, $m_{\widetilde{G}} \gtrsim 10$ TeV, so that

gravitinos decay before the onset of BBN. Then, overproduction of dark matter can be avoided by requiring an axino LSP with mass $m_{\tilde{a}} \sim 0.1 - 1$ MeV. Neutralinos produced either thermally or via gravitino decay will themselves decay typically to states such as $\tilde{a}\gamma$, so that the dark matter abundance is reduced by a factor $m_{\tilde{a}}/m_{\widetilde{Z}_1}$ [26]. The bulk of dark matter then resides in thermally produced axinos and/or in axions produced from vacuum mis-alignment. By driving up the value of PQ breaking scale f_a/N, thermal production of axinos is suppressed, and higher values of T_R are required to maintain a total axino plus axion relic abundance of $\Omega_{a\tilde{a}}h^2 \sim 0.11$. To avoid overproduction of axions at high f_a/N, we adopted a small vacuum mis-alignment angle $\theta_i \sim 0.05$. However, the large values of $f_a/N \sim 10^{12} - 10^{13}$ GeV suppress the $\widetilde{Z}_1$ decay rate, thus interfering with BBN from a different avenue. Models with a high-mass, bino-like $\widetilde{Z}_1$ and low "apparent" $\Omega^{app}_{\widetilde{Z}_1}h^2$ can avoid the BBN bounds, and allow T_R values in excess of 10^{10} GeV to be attained. As we showed, such conditions with $m_{\widetilde{G}} \sim 10 - 30$ TeV can be reached in Effective SUSY [19, 20] or mirage-unification SUSY breaking [21] models.

A related scenario to reconcile thermal leptogenesis with the gravitino problem — using mixed axion/axino dark matter — was proposed much earlier by Asaka and Yanagida (AY) [22]. Their proposal was to work within the context of the PQMSSM, but with a sparticle mass hierarchy $m(\text{sparticle}) > m_{\widetilde{G}} > m_{\tilde{a}}$. In this case, the couplings of MSSM sparticles to axinos are larger than the couplings to gravitinos, so that the long-lived decays to gravitino are bypassed, and the sparticles are assumed to decay to an axino LSP shortly before the onset of BBN. Furthermore, thermally produced gravitinos decay inertly via $\widetilde{G} \to a\tilde{a}$ and so do not disrupt BBN. Reheat temperatures as high as $T_R \sim 10^{15}$ were claimed to be possible.

In this paper, we re-visit the AY scenario, incorporating several improvements into our analysis. In particular, we implement

1. the latest astrophysically measured value of [23]

$$\Omega_{\rm DM}h^2 = 0.1123 \pm 0.0035 \quad \text{at } 68\% \text{ CL}; \tag{1.1}$$

2. the latest calculations for thermal production of gravitinos and axinos;

3. vacuum-misalignment production of axions as an element of the dark matter abundance;

4. the latest BBN constraints on late decaying particles; and finally

5. a careful treatment of entropy production from late decaying saxions.

The re-analysis of the AY scenario taking into account points 1.–4. is presented in Sec. 2, while entropy injection from saxion decay is discussed in detail in Sec. 3. In Sec. 4, we present our final conclusions and consequences of the AY scenario for LHC physics and dark matter searches.

2. Relic density of mixed axion/axino DM in the AY scenario

2.1 MSSM parameters

The only relevant MSSM parameters for our analysis are the $\widetilde{Z}_1$ and $\widetilde{G}$ masses $m_{\widetilde{Z}_1}$ and $m_{\widetilde{G}}$, the $\widetilde{Z}_1$ bino component $v_4^{(1)}$ in the notation of [6], and the $\widetilde{Z}_1$ abundance after freeze-out $\Omega_{\widetilde{Z}_1}$. The remaining of the MSSM parameters only impact the running of the gauge couplings and the value of $\Omega_{\widetilde{G}}$, which depend on all the gaugino masses (see Eq. (2.5) below). However, as shown below, in the AY scenario with $T_R \gtrsim 10^9$ GeV, the contribution from $\widetilde{G} \to a\tilde{a}$ decay to the dark matter relic density is negligible. Thus the dependence on the entire SUSY spectrum is very mild.

For illustration we will use a generic mSUGRA scenario with $m_0 = 1000$ GeV, $m_{1/2} = 1000$ GeV, $A_0 = 0$, $\tan\beta = 55$ and $\mu > 0$, which gives $m_{\widetilde{Z}_1} = 430$ GeV and $\Omega_{\widetilde{Z}_1} = 0.04$, but treat $m_{\widetilde{Z}_1}$ and $\Omega_{\widetilde{Z}_1}$ as free parameters throughout most of the numerical analysis. The bino component of the $\widetilde{Z}_1$ wavefunction is important, since it determines the $\widetilde{Z}_1 - \tilde{a}$ coupling. For simplicity we will assume a purely bino neutralino, which is valid for a large portion of the mSUGRA parameter space. We also take $m_{\widetilde{G}} = m_{\widetilde{Z}_1}/2$ and $m_{\tilde{a}} < m_{\widetilde{G}}$ in order to have an axino LSP with a gravitino NLSP.

2.2 Mixed axion/axino abundance calculation

Here, we consider four mechanisms for dark matter production in the AY scenario.

- If the reheat temperature T_R exceeds the axino decoupling temperature

$$T_{dcp} = 10^{11}\ \text{GeV} \left(\frac{f_a/N}{10^{12}\ \text{GeV}}\right)^2 \left(\frac{0.1}{\alpha_s}\right)^3, \tag{2.1}$$

  axinos will be in thermal equilibrium, with an abundance given by

$$\Omega_{\tilde{a}}^{TE} h^2 \simeq 0.38 \left(\frac{m_{\tilde{a}}}{1\ \text{keV}}\right). \tag{2.2}$$

  To avoid overproducing axino dark matter, the RTW bound [25] then implies that $m_{\tilde{a}} < 0.3$ keV.

  In the case where $T_R < T_{dcp}$, the axinos are never in thermal equilibrium in the early universe. However, they can still be produced thermally via radiation off of particles that are in thermal equilibrium [27, 28]. Here, we adopt a recent calculation of the thermally produced (TP) axino abundance from Strumia [29]:

$$\Omega_{\tilde{a}}^{\text{TP}} h^2 = 1.24 g_3^4 F(g_3) \frac{m_{\tilde{a}}}{\text{GeV}} \frac{T_R}{10^4\ \text{GeV}} \left(\frac{10^{11}}{f_a/N}\right)^2, \tag{2.3}$$

  with $F(g_3) \sim 20 g_3^2 \ln\frac{3}{g_3}$, and g_3 is the strong coupling constant evaluated at $Q = T_R$.

- In supersymmetric scenarios with a quasi-stable neutralino, the $\widetilde{Z}_1$s will be present in thermal equilibrium in the early universe, and will freeze out when the expansion rate exceeds their interaction rate, at a temperature roughly $T_{fo} \sim m_{\widetilde{Z}_1}/20$. The

present day abundance can be evaluated by integrating the Boltzmann equation. Several computer codes are available for this computation. Here we use the code IsaReD [30], a part of the Isajet/Isatools package [31, 32].

In our case, each neutralino will undergo decay to the stable axino LSP, via decays such as $\widetilde{Z}_1 \to \tilde{a}\gamma$. Neutralinos may also decay via *e.g.* $\widetilde{Z}_1 \to \widetilde{G}\gamma$, but these modes are suppressed by $1/m_{Pl}^2$ rather than $1/(f_a/N)^2$, and so the decay to gravitinos is suppressed (one of the hallmarks of the AY scenario). Thus, the non-thermally produced (NTP) axinos will inherit the thermally produced neutralino number density, and we will simply have [27]

$$\Omega_{\tilde{a}}^{\widetilde{Z}} h^2 = \frac{m_{\tilde{a}}}{m_{\widetilde{Z}_1}} \Omega_{\widetilde{Z}_1}^{TP} h^2. \tag{2.4}$$

- Since here we are attempting to generate reheat temperatures $T_R \gtrsim 10^9$ GeV, we must also include in our calculations the thermal production of gravitinos in the early universe. We adopt the calculation of Pradler and Steffen in Ref. [33], who have estimated the thermal gravitino production abundance as

$$\Omega_{\widetilde{G}}^{\rm TP} h^2 = \sum_{i=1}^{3} \omega_i g_i^2(T_R) \left(1 + \frac{M_i^2(T_R)}{3m_{\widetilde{G}}^2}\right) \ln\left(\frac{k_i}{g_i(T_R)}\right) \left(\frac{m_{\widetilde{G}}}{100\ \text{GeV}}\right) \left(\frac{T_R}{10^{10}\ \text{GeV}}\right), \tag{2.5}$$

  where $\omega_i = (0.018, 0.044, 0.117)$, $k_i = (1.266, 1.312, 1.271)$, g_i are the gauge couplings evaluated at $Q = T_R$ and M_i are the gaugino masses also evaluated at $Q = T_R$. For the temperatures we are interested in, this agrees within a factor of about 2 with the more recent calculation by Rychkov and Strumia [33], which is sufficient for our purposes.

  Since the only kinematically allowed gravitino decay mode is to an axion plus an axino LSP, the abundance of axinos from gravitino production is given by

$$\Omega_{\tilde{a}}^{\widetilde{G}} h^2 = \frac{m_{\tilde{a}}}{m_{\widetilde{G}}} \Omega_{\widetilde{G}}^{TP} h^2, \tag{2.6}$$

  while the abundance of axions from gravitino production is given by

$$\Omega_{a}^{\widetilde{G}} h^2 = \frac{m_{a}}{m_{\widetilde{G}}} \Omega_{\widetilde{G}}^{TP} h^2. \tag{2.7}$$

  For axino masses in the MeV range and gravitino masses in the TeV range, the prefactor above is extremely small, making the contribution from gravitino decays to the axino relic abundance negligible, what allows us to evade overproduction of dark matter via thermal gravitino production.

- Here, we consider the scenario where the PQ symmetry breaks before the end of inflation, so that a nearly uniform value of the axion field $\theta_i \equiv a(x)/(f_a/N)$ is expected throughout the universe. The axion field equation of motion implies that the axion field stays relatively constant until temperatures approach the QCD scale

$T_{QCD} \sim 1$ GeV. At this point, the temperature-dependent axion mass term turns on, and a potential is induced for the axion field. The axion field rolls towards its minimum and oscillates, filling the universe with low energy (cold) axions. The expected axion relic density via this vacuum mis-alignment mechanism is given by [34]

$$\Omega_a h^2 \simeq 0.23 f(\theta_i)\theta_i^2 \left(\frac{f_a/N}{10^{12}\ \text{GeV}}\right)^{7/6} \tag{2.8}$$

where $0 < \theta_i < \pi$ and $f(\theta_i)$ is the so-called anharmonicity factor. Visinelli and Gondolo [34] parametrize the latter as $f(\theta_i) = \left[\ln\left(\frac{e}{1-\theta_i^2/\pi^2}\right)\right]^{7/6}$. The uncertainty in $\Omega_a h^2$ from vacuum mis-alignment is estimated as plus-or-minus a factor of three.

In this paper, we will evaluate the mixed axion/axino relic density from the above four sources:

$$\Omega_{a\tilde{a}} h^2 = \Omega_{\tilde{a}}^{\rm TP} h^2 + \Omega_{\tilde{a}}^{\widetilde{Z}} h^2 + \Omega_{\tilde{a}}^{\widetilde{G}} h^2 + \Omega_a^{\widetilde{G}} h^2 + \Omega_a h^2. \tag{2.9}$$

Over much of parameter space, if $m_{\tilde{a}}$ is taken to be of order the MeV scale or below, then the contributions $\Omega_{\tilde{a}}^{\widetilde{G}}$, $\Omega_{\tilde{a}}^{\widetilde{Z}_1}$ and $\Omega_a^{\widetilde{G}}$ are subdominant.

In Fig. 1, we illustrate in frame *a*) the relative importance of the four individual contributions as a function of f_a/N, for $\Omega_{\widetilde{Z}_1} h^2 = 10$, $m_{\widetilde{Z}_1} = 430$ GeV and $m_{\widetilde{G}} = 0.5 m_{\widetilde{Z}_1}$. For the axion/axino sector we take $\theta_i = 0.05$ and $m_{\tilde{a}} = 100$ keV. The value of T_R is adjusted such that $\Omega_{a\tilde{a}} h^2 = 0.1123$. Low values of θ_i suppress axion production and allow higher values of f_a/N to be probed; the higher values of f_a/N suppress thermal axino production, thus allowing for higher T_R values to compensate.

For low f_a/N values, the TP axino contribution is dominant. But as f_a/N increases, the axion component grows. For higher values of f_a/N, the vacuum-misalignment produced axion component dominates, and the dark matter is predominantly composed of cold axions. The contribution of axino dark matter from $\widetilde{Z}_1$ and $\widetilde{G}$ decays are always negligible in this case.

In frame *b*) of Fig. 1, we show the value of T_R which is needed to enforce the total abundance of mixed axion/axino dark matter to be equal to $\Omega_{a\tilde{a}} h^2 = 0.1123$. We show cases for $m_{\tilde{a}} = 0.1$ and 1 MeV. As f_a/N increases, the axino-matter coupling decreases, and one would expect the thermal production of axinos to decrease. Since we enforce $\Omega_{a\tilde{a}} h^2 = 0.1123$, then higher values of T_R are needed to compensate and enhance the thermal production of axinos [35] (and gravitinos). We see that the value of T_R can be pushed to over 10^9 GeV for $m_{\tilde{a}} = 1$ MeV, and to over 10^{10} GeV for $m_{\tilde{a}} = 0.1$ MeV, thus allowing high enough T_R for thermal leptogenesis.

2.3 Constraint from cold dark matter

Depending on its mass, the axino might constitute warm (WDM) or hot (HDM) dark matter; the latter possibilities are severely constrained by the matter power spectrum and reionization [27,36] (see also [37,38]). We consider axinos with mass $1-100$ keV as mostly WDM, and axinos with mass < 1 keV as mostly HDM. Since these bounds on the amount of WDM/HDM are model dependent [36], we do not impose strict WDM/HDM constraints

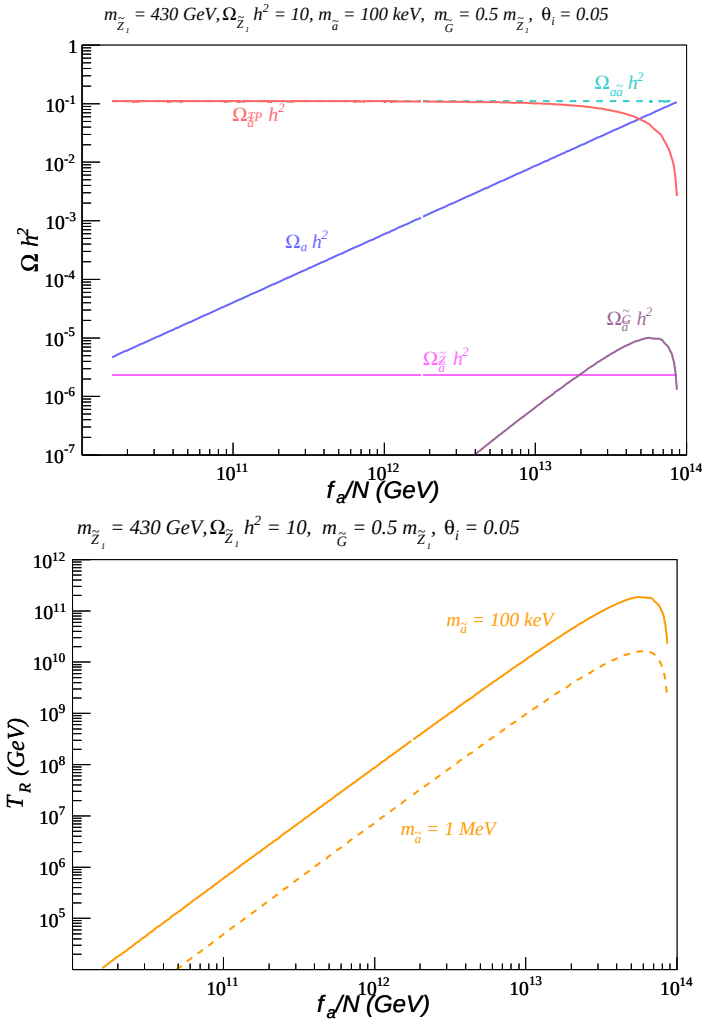

Figure 1: Upper frame: Contribution of axions and TP and NTP axinos to the DM density as a function of the PQ breaking scale f_a/N, for $m_{\widetilde{Z}_1} = 430$ GeV, $\Omega_{\widetilde{Z}_1} h^2 = 10$, $m_{\tilde{a}} = 100$ keV and $\theta_i = 0.05$; T_R is adjusted such that $\Omega_{a\tilde{a}} h^2 = 0.1123$. We assume $m_{\widetilde{G}} = m_{\widetilde{Z}_1}/2$. Lower frame: the value of T_R that is needed to achieve $\Omega_{a\tilde{a}} h^2 = 0.1123$ for $m_{\tilde{a}} = 0.1$ and 1 MeV.

on our results. However, for guidance, we will keep track of PQMSSM parameter points with potentially too large WDM and/or HDM components[1]: As in [12], we disfavour points with

$$\begin{aligned} &\Omega_{\tilde{a}}/\Omega_{a\tilde{a}} > 0.2 \quad \forall\ 1\ \text{keV} \leq m_{\tilde{a}} < 100\ \text{keV}, \quad \text{(WDM)} \\ &\Omega_{\tilde{a}}/\Omega_{a\tilde{a}} > 0.01\ \forall\ m_{\tilde{a}} < 1\ \text{keV}, \quad \text{(HDM)} \end{aligned} \tag{2.10}$$

where $\Omega_{\tilde{a}} = \Omega_{\tilde{a}}^{TP} + \Omega_{\tilde{a}}^{\widetilde{G}} + \Omega_{\tilde{a}}^{\widetilde{Z}}$. This is rather conservative. A rough estimate based on the neutrino mass limit [38] from cosmological data, $\sum m_\nu < 0.41$ to 0.44 eV, gives that up to 4–5% HDM contribution could be acceptable. Moreover, Boyarsky *et al.* in [37] found that in case of a thermal relic (TR), 100% WDM is allowed for $m_{\rm TR} \geq 1.7$ keV, while for

[1] Axions produced from gravitino decay will also constitute HDM. However, since its contribution to the total DM density is suppressed by $m_a/m_{\widetilde{G}}$, it can be safely neglected.

$m_{\rm TR} = 1.1$ keV as much as 40% WDM is allowed at 95% CL. We will also indicate these bounds, which are considerably weaker than Eq. (2.10).

2.4 Constraints on $\widetilde{Z}_1$ decay from BBN

The AY scenario naturally avoids BBN constraints on late decaying gravitinos by assuming the mass relation $m(\text{sparticle}) > m_{\widetilde{G}} > m_{\tilde{a}}$, so that the $\widetilde{G}$ decays inertly 100% of the time into $a\tilde{a}$. However, by searching for PQMSSM parameters which allow $T_R \gtrsim 2 \times 10^9$ GeV while avoiding overproduction of mixed axino/axion dark matter (the latter requires large $f_a/N \sim 10^{12}$ GeV and small θ_i), we have pushed the $\widetilde{Z}_1$ lifetime uncomfortably high, so that its hadronic decays in the early universe now have the potential to disrupt BBN. The $\widetilde{Z}_1$ lifetime and hadronic branching fraction is calculated in Ref. [12, 27].

Constraints from BBN on hadronic decays of long-lived neutral particles in the early universe have been calculated in Ref's [39–41]. Here, we adopt the results from Jedamzik [41]. The BBN constraints arise due to injection of high energy hadronic particles into the thermal plasma during or after BBN. The constraints depend on three main factors:

- The abundance of the long-lived neutral particles. In Ref. [41], this is given by $\Omega_X h^2$ where X is the long-lived neutral particle which undergoes hadronic decays. In our case, where the long-lived particle is the lightest neutralino which decays to an axino LSP, this is just given by the usual thermal neutralino abundance $\Omega_{\widetilde{Z}_1} h^2$, as calculated by IsaReD [30].

- The lifetime τ_X of the long-lived neutral particle. The longer-lived X is, the greater its potential to disrupt the successful BBN calculations. In our case $\tau_X = \tau_{\widetilde{Z}_1} \propto (f_a/N)^2/m^3_{\widetilde{Z}_1}$.

- The hadronic branching fraction B_h of the long-lived neutral particle. If this is very small, then very little hadronic energy will be injected, and hence the constraints should be more mild.

From the above list, we see that BBN directly constrains the MSSM parameters ($\Omega_{\widetilde{Z}_1} h^2$ and $m_{\widetilde{Z}_1}$) of the PQMSSM model. The constraints also depend on f_a, since its value directly affects $\tau_{\widetilde{Z}_1}$. The BBN constraints are shown in Fig. 9 (for $m_X = 1$ TeV) and Fig. 10 (for $m_X = 100$ GeV) of Ref. [41], as contours in the τ_X *vs.* $\Omega_X h^2$ plane, with numerous contours for differing B_h values ranging from 10^{-5} to 1. For $B_h \sim 0.1$, for instance, and very large values of $\Omega_X h^2 \sim 10 - 10^3$, the lifetime τ_X must be $\lesssim 0.1$ sec, or else the primordial abundance of ^4He is disrupted. If $\Omega_X h^2$ drops below ~ 1, then much larger values of τ_X up to ~ 100 sec are allowed. If one desires a long-lived hadronically decaying particle in the early universe with $\tau_X \gtrsim 100$ sec, then typically much lower values of $\Omega_X h^2 \sim 10^{-6} - 10^{-4}$ are required.

We have digitized the constraints of Ref. [41], implementing extrapolations for cases intermediate between values of parameters shown, so as to approximately apply the BBN constraints to the AY scenario with a long-lived neutralino decaying during BBN. The results are shown in Fig. 2, as a function of $m_{\widetilde{Z}_1}$. From Fig. 1*b)*, we have $T_R > 10^9$ GeV for

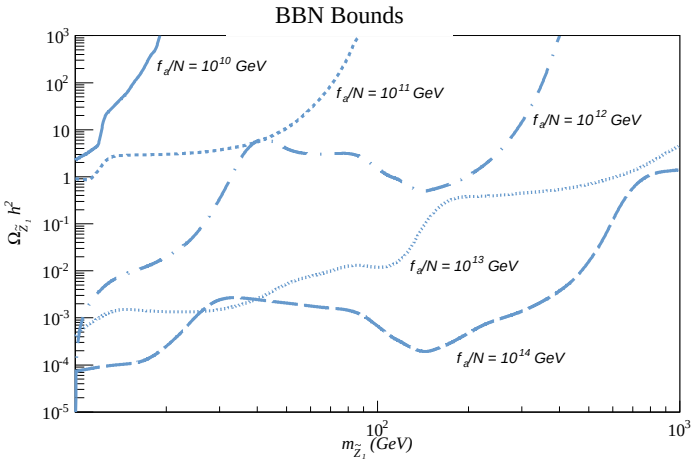

Figure 2: BBN bounds on late decaying neutralinos ($\widetilde{Z}_1 \to Z/\gamma + \tilde{a}$) from Ref. [41] as a function of $m_{\widetilde{Z}_1}$ for different values of f_a/N, assuming a bino $\widetilde{Z}_1$ and $m_{\widetilde{Z}_1} \gg m_{\tilde{a}}$. The values of $\Omega_{\widetilde{Z}_1} h^2$ above the curves are excluded by BBN constraints.

$f_a/N \sim 10^{13}$ GeV. From Fig. 2, we see that, for $m_{\widetilde{Z}_1} \sim 400$ GeV and $f_a/N = 10^{13}$ GeV, we need $\Omega_{\widetilde{Z}_1} h^2 < 0.4$ in order to satisfy the BBN bounds. In particular, the assumed value for $\Omega_{\widetilde{Z}_1} h^2$ (=10) in Fig. 1 only satisfies the BBN constraints for $f_a/N \lesssim 2 \times 10^{12}$ GeV or $T_R \lesssim 3 \times 10^8$ GeV. Therefore we see that the AY scenario with $T_R \gtrsim 10^9$ GeV requires quite low values of $\Omega_{\widetilde{Z}_1} h^2$ and/or a heavy $\widetilde{Z}_1$.

2.5 Scan over PQ parameters

The results of the last section were for a specific choice of the axino mass and θ_i values. Next, we examine which values of T_R are possible for arbitrary values of f_a, $m_{\tilde{a}}$ and θ_i. For now we keep the MSSM parameters ($\Omega_{\widetilde{Z}_1} h^2$ and $m_{\widetilde{Z}_1}$) fixed. As discussed in the previous section, the BBN constraints in general require low $\Omega_{\widetilde{Z}_1} h^2$ and high $m_{\widetilde{Z}_1}$. We therefore assume $\Omega_{\widetilde{Z}_1} h^2 = 0.04$ and $m_{\widetilde{Z}_1} = 430$ GeV, which are values consistent with, e.g., an mSUGRA point near the apex of the Higgs funnel region. To probe the full PQ parameter space we perform a random scan over the PQ parameters in the range

$$\begin{aligned} m_{\tilde{a}} &\in [10^{-7},\ 10]\ \text{GeV}\,, \\ f_a/N &\in [10^8,\ 10^{15}]\ \text{GeV}\,, \\ \theta_i &\in [0,\ \pi]\,. \end{aligned} \tag{2.11}$$

and calculate the value of T_R which is needed to enforce $\Omega_{a\tilde{a}} h^2 = 0.1123$. The results of our scan are shown in Fig. 3, where we plot the derived value of T_R versus PQ breaking scale f_a/N. In the plot, dark blue and dark red points have mainly CDM with at most 20% WDM and at most 1% HDM admixture, c.f. Section 2.3. The light blue and light red points have higher values of WDM or HDM. The red points are excluded by bounds derived from Ref. [41] on late decaying neutralinos which could destroy the succesful predictions of BBN. Blue points are allowed by BBN constraints. Applying the WDM bounds of

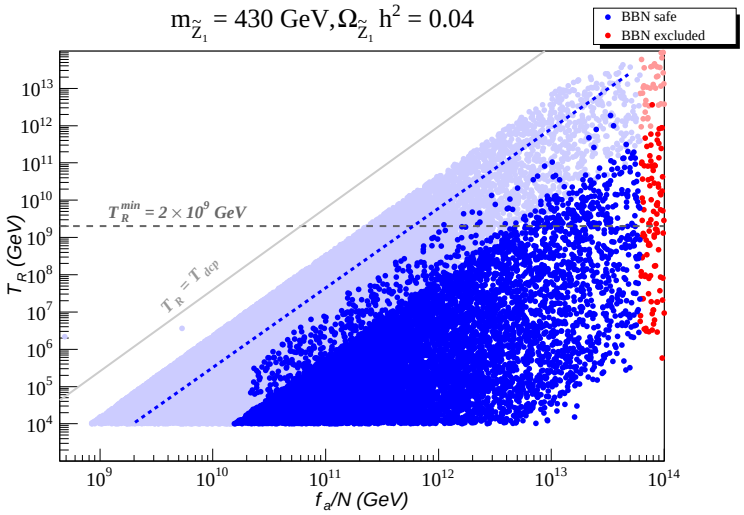

Figure 3: Allowed and disallowed points in the f_a *vs.* T_R plane for $m_{\widetilde{Z}_1} = 430$ GeV and $\Omega_{\widetilde{Z}_1}h^2 = 0.04$, including BBN constraints on late $\widetilde{Z}_1$ decay. Dark blue points have mainly CDM with at most 20% WDM and at most 1% HDM admixture; the dashed blue line indicates the WDM limit by Boyarsky *et al.* [37] and up to 5% HDM

Boyarsky *et al.* [37] for a thermal relic and allowing up to 5% HDM, the boundary between dark and light blue points moves left to the dashed blue line.

We do see that a number of dark blue points with mainly CDM, and which also respect BBN bounds, can be generated with $T_R > 2\times10^9$ GeV. These thermal leptogenesis-consistent points all require $f_a/N \gtrsim 10^{12}$ GeV (or $f_a/N \gtrsim 6\times10^{11}$ GeV with weaker WDM/HDM requirements).

In Fig. 4, we show the same scan in the θ_i *vs.* T_R plane. Here, we see that the CDM/BBN consistent points with high T_R all need rather small values of axion misalignment angle $\theta_i \lesssim 0.5$. This is needed since, at large T_R, large f_a/N is necessary to suppress overproduction of axinos, while small θ_i is needed to suppress over-production of axions.

In Fig. 5, we show the same PQMSSM parameter scan for $m_{\widetilde{Z}_1} = 430$ GeV and $\Omega_{\widetilde{Z}_1}h^2 = 0.04$, but in the $\Omega_a h^2$ *vs.* T_R plane. Here, we see that the CDM/BBN consistent points with high T_R can have both large and small values of $\Omega_a h^2$. Solutions with $\Omega_a h^2 \sim 0.1$ usually have very light axinos (to suppress $\Omega_{\tilde{a}}h^2$) and moderate θ_i values. Solutions with $\Omega_a h^2 \lesssim 0.4$ usually have heavier axinos and small θ_i.

While the results of the previous figures are restricted to specific values of $m_{\widetilde{Z}_1}$ and $\Omega_{\widetilde{Z}_1}h^2$, the overall scheme is much more general. The lesson here is that the AY scenario for reconciling thermal leptogenesis with the gravitino problem can work provided certain conditions on SUSY models are met. These conditions are rather similar to those needed by the large $m_{3/2}$ scenario put forth in Ref. [12]. After adopting a model with a sparticle mass hierarchy of $m(\text{sparticles}) > m_{\widetilde{G}} > m_{\tilde{a}}$, with $m_{\tilde{a}}$ ~MeV scale and $m_{\widetilde{G}} \sim M_{\text{weak}}$, one needs the following features:

- To allow for $T_R > 2\times10^9$ GeV, one must suppress thermal production of axinos via

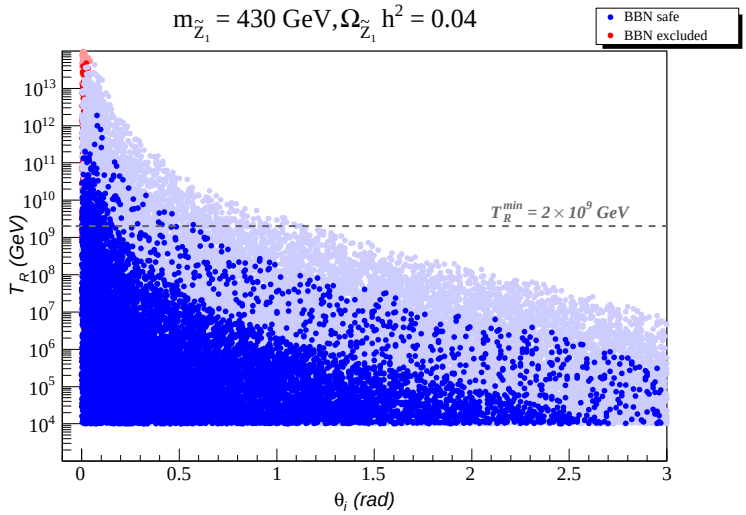

Figure 4: Allowed and disallowed points in the θ_i *vs.* T_R plane for $m_{\widetilde{Z}_1} = 430$ GeV and $\Omega_{\widetilde{Z}_1}h^2 = 0.04$, including BBN constraints on late $\widetilde{Z}_1$ decay.

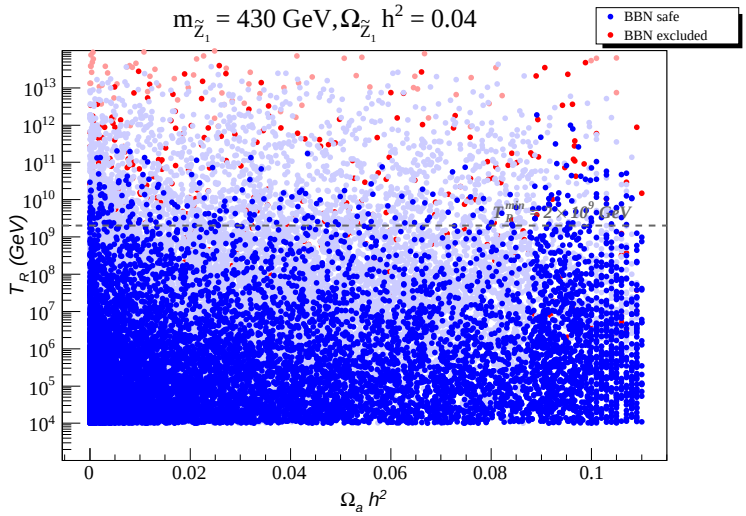

Figure 5: Allowed and disallowed points in the $\Omega_a h^2$ *vs.* T_R plane for $m_{\widetilde{Z}_1} = 430$ GeV and $\Omega_{\widetilde{Z}_1}h^2 = 0.04$, including BBN constraints on late $\widetilde{Z}_1$ decay.

a large value of $f_a/N \gtrsim 10^{12}$ GeV.

- To suppress overproduction of axions one must adopt a lower range of mis-alignment angle $\theta_i \lesssim 0.5$ (or $\theta_i \lesssim 0.8$ taking into account the factor 3 uncertainty in Eq. (2.8)) .
- The large value of f_a/N increases the $\widetilde{Z}_1$ lifetime, which brings in BBN constraints on late-decaying neutral particles. To avoid BBN bounds, it helps to invoke 1. a bino-like $\widetilde{Z}_1$ so that $v_4^{(1)} \sim 1$, 2. a low apparent neutralino relic abundance $\Omega_{\widetilde{Z}_1}^{app}h^2 \lesssim 1$ and 3. a large value of $m_{\widetilde{Z}_1}$ to help suppress the $\widetilde{Z}_1$ lifetime.

These conditions are illustrated in a more model independent way in Fig. 6. Here, we

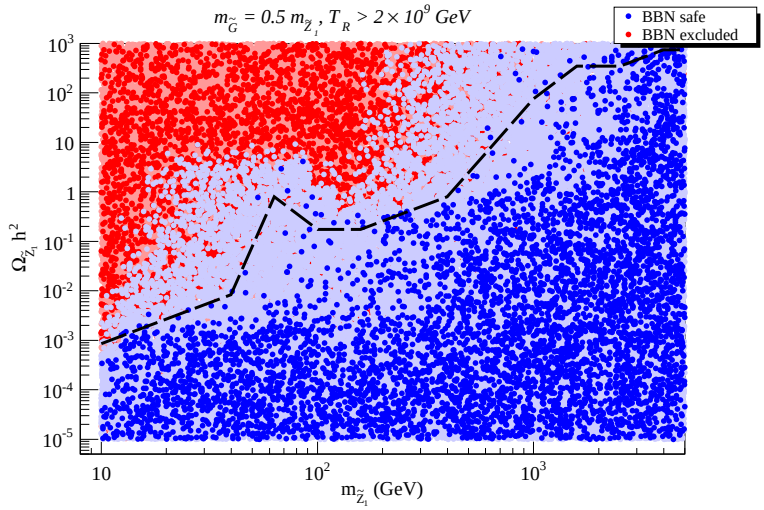

Figure 6: Allowed and disallowed points in the $\Omega_{\widetilde{Z}_1}h^2$ *vs.*$m_{\widetilde{Z}_1}$ plane for a general scan over SUSY models with a bino $\widetilde{Z}_1$. For all points, we require $T_R > 2\times 10^9$ GeV and assume $m_{\widetilde{G}} = m_{\widetilde{Z}_1}/2$. Dark blue points are consistent with BBN and have mainly CDM with at most 20% WDM and/or 1% HDM admixture. The region below the dashed line represents the MSSM parameter space where 99% of the DM/BBN consistent solutions lie when applying weaker WDM/HDM requirements as discussed in the text.

assume the AY mass hierarchy, but extend our previous scan to the whole PQMSSM parameter space:

$$\begin{aligned} m_{\tilde{a}} &\in [10^{-7},\ 10]\ \text{GeV}\,, \\ f_a/N &\in [10^{8},\ 10^{15}]\ \text{GeV}\,, \\ \theta_i &\in [0,\ \pi]\,, \\ \Omega_{\widetilde{Z}_1}h^2 &\in [10^{-5}, 10^{3}]\,, \\ m_{\widetilde{Z}_1} &\in [10, 10^{4}]\ \text{GeV}\,. \end{aligned}$$

As before, we assume $m_{\widetilde{G}} = m_{\widetilde{Z}_1}/2$ and the blue points are BBN-allowed, while red points violate BBN bounds. The dashed line indicates the boundary blow which 99% of the DM/BBN consistent solutions lie when applying weaker WDM/HDM requirements (WDM limit according to Boyarsky *et al.* [37] and up to 5% HDM, cf. Fig. 3) This line can be interpreted as a natural upper bound for $\Omega_{\widetilde{Z}_1}h^2$ as a function of $m_{\widetilde{Z}_1}$. From this we see that models with $m_{\widetilde{Z}_1} \lesssim 10$ GeV require $\Omega_{\widetilde{Z}_1}h^2 \lesssim 10^{-3}$, while values of $\Omega_{\widetilde{Z}_1}h^2$ as high as 10^3 can be consistent with thermal leptogenesis if the neutralino is in the TeV range.

3. Dilution of DM by entropy production from saxion decay

Up to this point, we have neglected an important element of the axion supermultiplet, namely the spin-0 saxion field $s(x)$ which is expected to obtain a soft SUSY breaking mass at the GUT scale of $m_s \sim m_0$. In the same way as axinos, saxions can be produced in thermal equilibrium (if $T_R > T_{dcp}$) or out of equilibrium from scatterings of particles in

the plasma (if $T_R < T_{dcp}$). However a second mechanism of saxion production is also possible [45]. After supersymmetry breaking, the saxion potential $V(s)$ develops a global minimum, causing the saxion field to coherently oscillate around its minimum. This coherent oscillation can have a large energy density, which contributes to the total saxion energy density if $T_R < T_{dcp}$. However, if $T_R > T_{dcp}$, the coherent oscillating saxions will couple to the thermal plasma and thermalize.

Once the saxions decouple from the thermal plasma (at $T = T_{dcp}$) and become non-relativistic (at $T \sim m_s$), their energy density (ρ_s) scales as T^3 (or R^{-3}), while the thermal plasma's energy density (ρ_{rad}) scales as T^4 (or R^{-4}). If the saxion lifetime is sufficiently long, at some temperature T_e, we will have $\rho_s > \rho_{rad}$ and the universe will become temporarily matter dominated until the saxions decay.

Being a R-parity even state, the saxion can decay to standard model states or pairs of sparticles. Since we assume $m_s \sim m_0$, the decay into SUSY states will be kinematically suppressed and the saxion decays will mostly consist of SM particles Therefore the saxion decay products will thermalize in the thermal plasma, which is then "relatively reheated" [47] with respect to other decoupled particles, such as axinos. As a consequence, all particles decoupled from the thermal plasma during the saxion decay will have their number density diluted with respect to the thermal bath's. Below we introduce the relevant expressions necessary for computing this dilution factor (r) and in Sec. 3.3 we discuss how the inclusion of the saxion field impacts our previous results.

3.1 Saxion production and decay

As mentioned above, if T_R exceeds T_{dcp} in the early universe, saxions are produced in thermal equilibrium such that

$$Y_s m_s = \frac{\rho_s}{s} \simeq 10^{-3} \frac{m_s}{\text{GeV}}, \tag{3.1}$$

where $s = 2\pi^2 g_* T^3/45$ is the plasma entropy density and Y_s is the saxion yield. For $T_R < T_{dcp}$, saxions can still be produced thermally, although to our knowledge a full calculation is not yet available. In Ref's [22] and [45], thermal saxion production is estimated to be

$$\frac{\rho_s}{s} \simeq 10^{-3} m_s T_R / T_{dcp} = m_s \left(\frac{T_R}{10^{14}\ \text{GeV}}\right) \left(\frac{10^{12}\ \text{GeV}}{f_a/N}\right)^2, \tag{3.2}$$

which we will adopt for our calculations.

In addition, saxions can be produced via coherent oscillations of the saxion field in the early universe. Although the exact mechanism depends on the saxion potential near the SUSY breaking scale, the energy density associated with the coherent oscillations can be parametrized by the initial saxion field strength, s_i. Natural values for s_i are $s_i \sim f_a$ or $s_i \sim M_{Pl}$. Unless stated otherwise, we will assume $s_i = f_a/N$. The saxion energy density is estimated for the case of very high values of T_R with $\Gamma_I > m_s$ (here, T_R is related to the inflaton decay width Γ_I as $T_R = (3/g_*\pi^3)^{1/4}(M_{Pl}\Gamma_I)^{1/2}$) as [45]

$$\frac{\rho_s}{s} \simeq 1.5 \times 10^{-5}\ \text{GeV} \left(\frac{m_s}{1\ \text{GeV}}\right)^{1/2} \left(\frac{(f_a/N)}{10^{12}\ \text{GeV}}\right)^2 \left(\frac{s_i}{(f_a/N)}\right)^2 \tag{3.3}$$

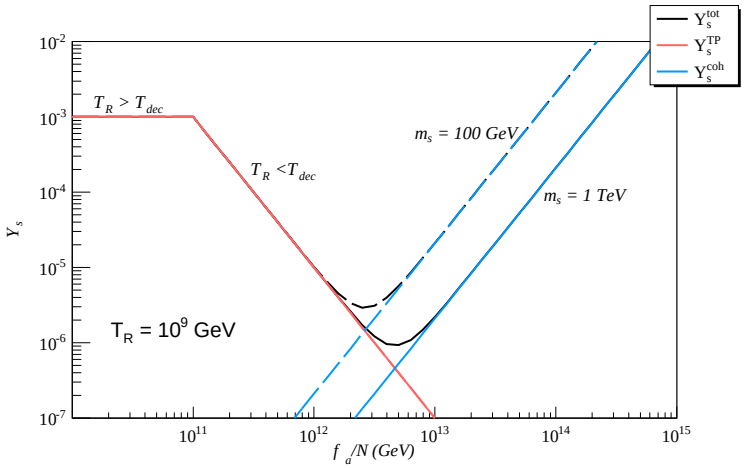

Figure 7: Saxion yield Y_s versus f_a/N for $T_R = 10^9$ GeV and $m_s = 0.1$ and 1 TeV. We assume $s_i/(f_a/N) = 1$.

while for $\Gamma_I < m_s$,

$$\frac{\rho_s}{s} \simeq 2.1 \times 10^{-9} \text{ GeV} \left(\frac{T_R}{10^5 \text{ GeV}}\right) \left(\frac{(f_a/N)}{10^{12} \text{ GeV}}\right)^2 \left(\frac{s_i}{(f_a/N)}\right)^2 . \tag{3.4}$$

The summed saxion abundance is then given by the thermal production if $T_R > T_{dcp}$ or by the sum of thermal production plus the abundance from coherent oscillations, if $T_R < T_{dcp}$.

As an example, we show in Fig. 7 the saxion yield Y_s versus f_a/N for $m_s = 0.1$ and 1 TeV and for $T_R = 10^9$ GeV. At low f_a/N, $T_R > T_{dcp}$, and saxions are produced in thermal equilibrium. Once T_{dcp} rises above T_R, thermal saxion production dominates, but decreases with increasing f_a/N until the point where saxion production from coherent oscilations dominates.

The saxion is an R-parity even state which is expected to dominantly decay into two gluons: $s \to gg$. The saxion decay width differs by factors of two in Ref's [46], [22] and [45]. By an independent calculation, we find

$$\Gamma(s \to gg) = \frac{\alpha_s^2 m_s^3}{32\pi^3 (f_a/N)^2}, \tag{3.5}$$

in agreement with [22]. The saxion may also decay (or not, model dependently) via $s \to aa$, and in the DFSZ [16] model, into $q\bar{q}$ or $\ell\bar{\ell}$. These latter decays are suppressed in the KSVZ model [15]. Saxion may also decay to $\widetilde{Z}_i\widetilde{Z}_j$, $\gamma\gamma$ and $\tilde{g}\tilde{g}$. For saxion decay to gluino pairs, we find

$$\Gamma(s \to \tilde{g}\tilde{g}) = \frac{\alpha_s^2 m_s m_{\tilde{g}}^2}{2\pi^3 (f_a/N)^2} \left(1 - \frac{4m_{\tilde{g}}^2}{m_s^2}\right)^{3/2} . \tag{3.6}$$

The two widths are compared in Fig. 8, where the $s \to gg$ decay is found to always dominate.

The temperature associated with saxion decay and entropy injection is given by [47]

$$T_s \simeq 0.78 g_*^{-1/4} \sqrt{\Gamma_s M_{Pl}}. \tag{3.7}$$

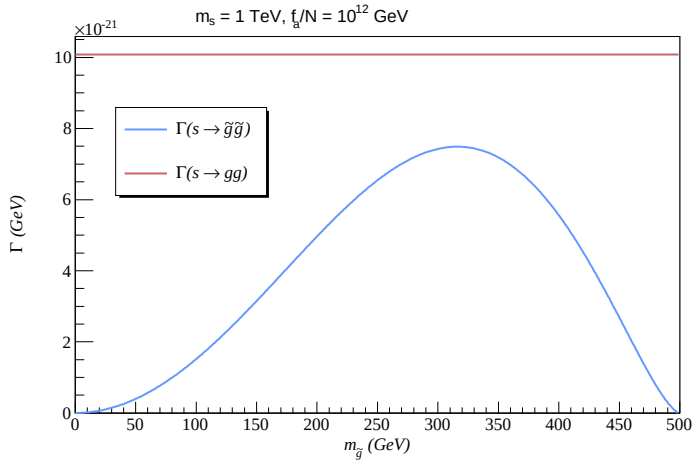

Figure 8: Decay widths for $s \to gg$ and $s \to \tilde{g}\tilde{g}$ as a function of $m_{\tilde{g}}$ for $f_a/N = 10^{12}$ GeV and $m_s = 1$ TeV.

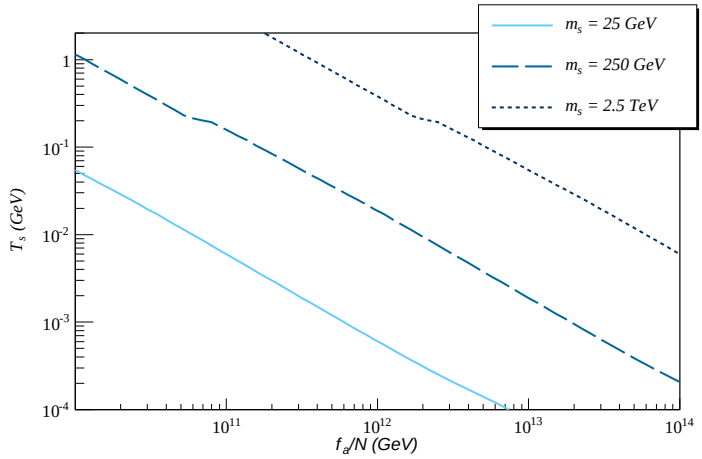

Figure 9: Temperature T_s at which saxions finish injecting entropy versus f_a/N for $m_s = 25,\ 250$ and 2500 GeV.

All the saxion decays essentially finish entropy injection by the time the universe cools to this value [47]. For simplicity, here we will assume the $\Gamma_s = \Gamma(s \to gg)$ so that our results are independent of $m_{\tilde{g}}$. Folding in the additional strong decay $s \to \tilde{g}\tilde{g}$ will result typically in a small increase in T_s. In Fig. 9, we plot the value T_s as a function of f_a/N for three different values of the saxion mass.

3.2 Entropy injection from saxion decay

Armed with expressions for the saxion production rate in the early universe, we next calculate the temperature T_e at which the saxion energy density in the universe equals the plasma energy density:

$$\rho_s(T_e) = \rho_{rad}(T_e) = \frac{\pi^2 g_*}{30} T_e^4. \tag{3.8}$$

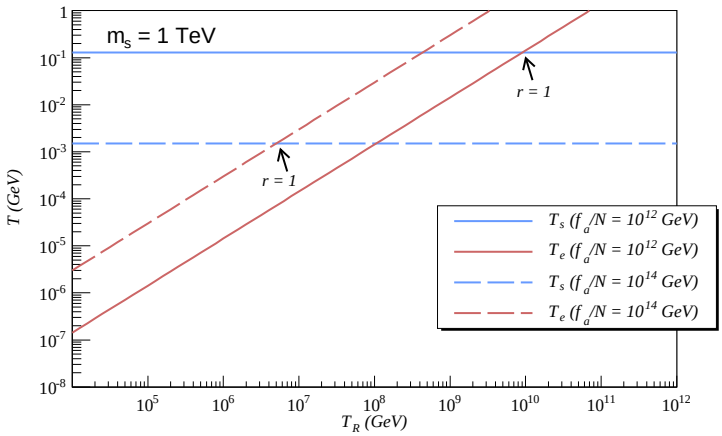

Figure 10: Temperatures T_s and T_e versus T_R for $f_a/N = 10^{12}$ and 10^{14} GeV and for $m_s = 1$ TeV.

Using $\rho_s = m_s Y_s s$ and $s = \frac{2\pi^2}{45} g_* T^3$, we find

$$T_e = \frac{4}{3} m_s Y_s. \tag{3.9}$$

If T_e exceeds T_s (*i.e.* if saxion domination occurs before saxion decay), then saxions dominate the energy density of the universe for $T_s \lesssim T \lesssim T_e$. In this case, saxion decays may inject significant entropy and dilute whatever abundances are present at temperature T_s. The situation is shown in Fig. 10, where we show the value of T_s (blue horizontal lines) and the value of T_e (red lines) for $f_a/N = 10^{12}$ and 10^{14} GeV. For T_R greater than the $r = 1$ intersection points, significant entropy injection can occur.

One condition on T_s is that $T_s \gtrsim 10$ MeV so the saxion decay does not disrupt standard BBN. If the conditions 10 MeV $< T_s$ and $T_e > T_s$ hold, then saxion decay can inject substantial entropy and dilute whatever relics are present and decoupled from the thermal plasma at the time of saxion decay ($T = T_s$). The ratio of entropy injection before and after a quasi-stable particle decay, for a matter dominated universe ($T_e > T_s$), has been calculated in Scherrer and Turner [47], and is given by

$$r = \frac{S_f}{S_i} \simeq 1.83 \bar{g}_*^{1/4} \frac{Y_s m_s}{(M_{Pl}\Gamma_s)^{1/2}} \sim \frac{T_e}{T_s}, \tag{3.10}$$

where $\bar{g}_*$ is the number of relativistic degrees of freedom averaged over the saxion decay period, which we approximate by $g_*(T_s)$. The above expression for r is only valid for $T_e > T_s$ (saxion dominated universe) or $r > 1$. However, if the saxion energy density never dominates the universe, the entropy injection is negligible [47]. Therefore we assume $r = 1$ (no entropy injection), if $T_e < T_s$.

Assuming Γ_s is dominated by the $s \to gg$ decay, we plot in Fig. 11*a*) the value of r in the (f_a/N) *vs.* T_R plane for $m_s = 0.1$, 1 and 10 TeV, assuming $s_i/(f_a/N) = 1$ (for production from coherent oscillations). The solid lines all maintain $T_s > 10$ MeV, while dashed lines violate this constraint. We see first that for $m_s = 100$ GeV, significant entropy

production only occurs for $f_a/N \lesssim 4\times 10^{11}$ GeV; for larger f_a/N, Γ_s is suppressed and the saxion lives long enough to decay during or after BBN. For $m_s = 1$ TeV, entropy injection can occur for $f_a/N \lesssim 10^{13}$ GeV.

If T_R lies below the $r = 1$ contours, then not much entropy is injected, but for high T_R, large entropy injection is possible and must be accounted for. The various contours of constant r initially increase with T_R. In this case, the saxion production is dominantly thermal. When the curves turn over, saxion production is dominated by coherent oscillations. In this case, as f_a/N increases, the saxion field strength also increases (since $s_i/(f_a/N)$ is fixed to 1), and much lower T_R values are allowed for substantial entropy production. Another noteworthy feature is that the contours of entropy production increase with T_R as m_s increases. Thus, the dilution of DM from saxion decay can be reduced by requiring rather heavy saxions. Finally, when we compare Fig. 3 to Fig. 11, we see that the range of $T_R \sim 10^9 - 10^{11}$ GeV for $f_a/N \sim 10^{12} - 10^{14}$ implies that entropy dilution from saxion decay needs to be accounted for in our calculations for the case where $s_i/(f_a/N) \sim 1$ and $m_s = m_0 = 1$ TeV.

In Fig. 11*b*), we plot again the entropy ratio contours, but this time taking $s_i/(f_a/N) = 0.1$. In this case, saxion production from coherent oscillations is suppressed by the smaller initial saxion field strength value. This expands the range of large T_R at high f_a/N where entropy injection is negligible. In cases such as these, the results of the previous section (and also Ref. [12]) remain viable, and entropy injection from saxion decay would be a negligible effect. From here on, we will assume $s_i/(f_a/N) = 1$.

As mentioned before, the entropy injection from late decaying saxions will dilute the number density of any particle decoupled from the thermal plasma at $T = T_s$. Therefore, depending on T_s, the saxion production and decay may dilute thermally produced axinos, gravitinos, the quasi-stable $\widetilde{Z}_1$s and sometimes the axions. To include this effect into our previous results, we adopt the following procedure:

- Calculate the thermal plus coherent oscillation yield of saxions Y_s in the early universe.
- Calculate the saxion decay temperature T_s.
- Calculate T_e and determine if saxions can dominate the universe ($T_e > T_s$).
- Calculate the final/initial entropy ratio r.
- If $r < 1$, then the entropy injection is negligible and our previous results hold,
- If $T_s < 10$ MeV and $r > 1$, then the point is excluded due to entropy injection during or after BBN.
- If $T_s > 10$ MeV and $r > 1$,
  - dilute thermally produced axinos by factor r.
  - dilute thermally produced gravitinos by r.
  - If $T_s < T_{QCD} = 1$ GeV, dilute mis-alignment produced axions by r.

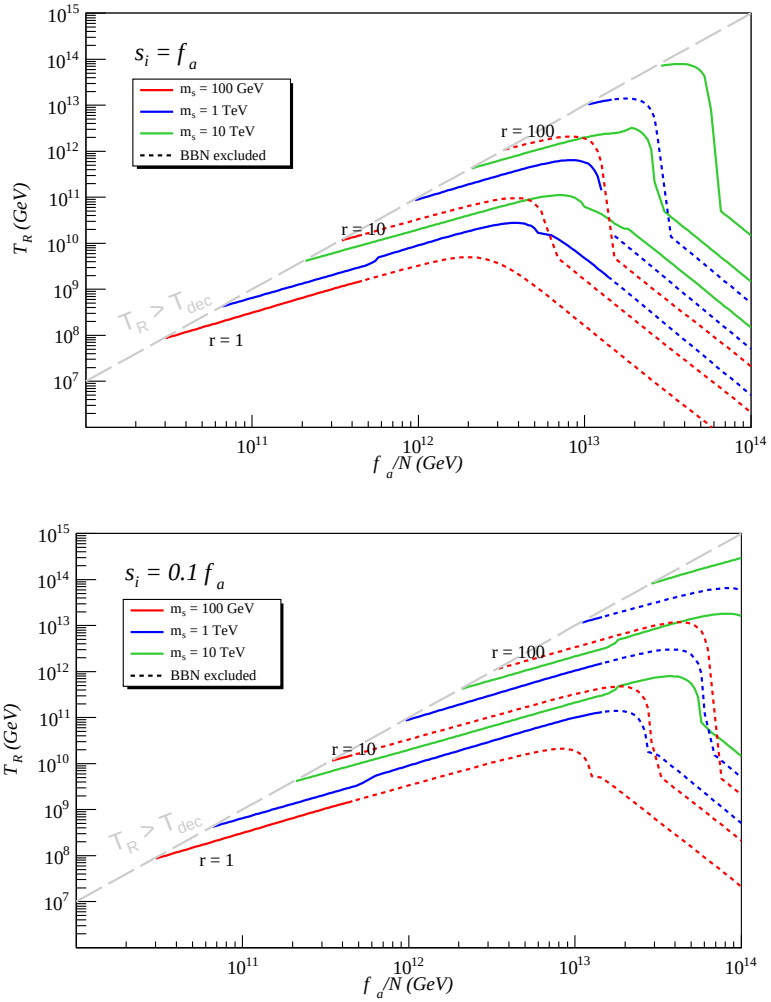

Figure 11: Ratio of entropy r before and after saxion decay in the f_a/N *vs.* T_R plane for $m_s = 0.1,\ 1,\ 10$ TeV and for *a)* $s_i/(f_a/N) = 1$ and *b)* $s_i/(f_a/N) = 0.1$. The dashed lines correspond to $T_{decay} < 10$ MeV, when the entropy from saxion decay is injected after the beginning of BBN; these regions are likely excluded.

– If $T_s < T_{fo} = m_{\tilde{Z}_1}/25$, dilute quasi-stable neutralinos by r. This condition can dilute axinos produced by neutralino decay, but also impacts the quasi-stable neutralino BBN bounds from Fig. 2.

Our first results are shown in Fig. 12 for the same PQMSSM parameters used in Fig. 1, but including saxion entropy injection with $m_s = 1$ TeV. In frame *a*), we plot the relic abundance of thermally produced axinos (red), axions (blue), gravitino produced axinos (lavender) and neutralino produced axinos (magenta). The value of T_R is always adjusted to maintain $\Omega_{a\tilde{a}} = 0.1123$, and is shown in frame *b*) for $m_{\tilde{a}} = 0.1$ and 1 MeV.

For low values of f_a/N, the relic abundance curves track the values shown in Fig. 1. In this case, T_R is much lower than the leptogenesis value 2×10^9 GeV, and the thermal yield

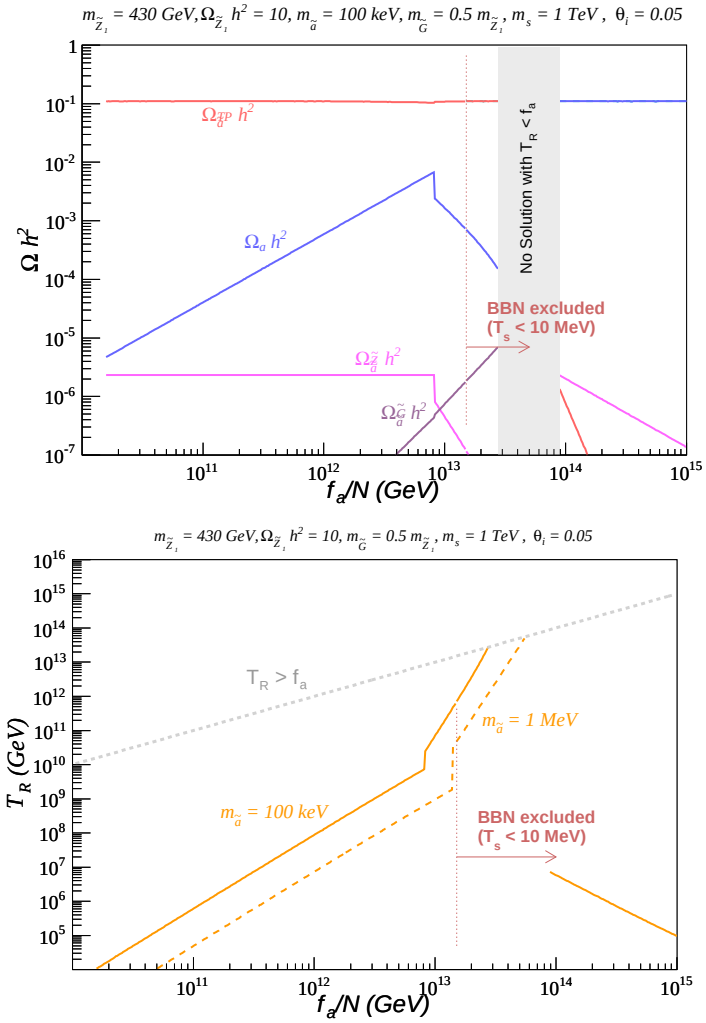

Figure 12: Upper frame a): Contribution of axions and TP and NTP axinos to the DM density as a function of the PQ breaking scale f_a/N, for $\Omega_{\widetilde{Z}_1} h^2 = 10$ and $m_{\widetilde{Z}_1} = 430$ GeV, with $m_{\tilde{a}} = 100$ keV and $\theta_i = 0.05$; T_R is adjusted such that $\Omega_{a\tilde{a}} h^2 = 0.1123$. We assume $m_s = m_0 = 1$ TeV and $m_{\widetilde{G}} = m_{\widetilde{Z}_1}/2$. Lower frame b): the value of T_R that is needed to achieve $\Omega_{a\tilde{a}} h^2 = 0.1123$ for $m_{\tilde{a}} = 0.1$ and 1 MeV.

of saxions is too low for significant entropy production. As f_a/N increases, the thermal axino production drops, and the value of T_R must compensate by increasing the thermal yield of axinos so that $\Omega_{a\tilde{a}} h^2 = 0.1123$ is maintained. At around $f_a/N \sim 10^{13}$ GeV, the value of T_s drops below T_e, and significant entropy production from saxion decay occurs. The entropy injection dilutes the thermal axino and also axion production, so that a sharp increase in T_R is needed to offset the dilution effect: the dark matter abundance remains dominated by thermal axino production. However, the axion abundance is independent of T_R, and so its dilution due to saxion decay is plain to see in frame a).

The value of T_R needed to maintain $\Omega_{a\tilde{a}} h^2 = 0.1123$ increases sharply until the regime $T_R > f_a/N$ is reached. For such high values of T_R, the PQ symmetry is restored during

re-heat, and re-broken during subsequent cooling. The universe should break into domains of different θ_i and s_i values (see *e.g.* M. Turner in Ref. [34]), and a modified treatment of dark matter will be needed. Therefore we neglect such solutions and impose the condition $T_R < f_a/N$ to our solutions.

As f_a/N increases even further, we move into the range where $T_s < 10$ MeV, and saxion decay might disrupt BBN. In this excluded region, two solutions to the restriction $\Omega_{a\tilde{a}}h^2 = 0.1123$ appear. The first has dark matter dominated by thermal axinos and ultra-high $T_R \gg f_a/N$ wherein the axinos and axions are severely diluted by saxion entropy production; these solutions are not exhibited on the plot. The second solution allows for much lower T_R values in which case dark matter is dominated by axion production, albeit with some dilution due to coherent oscillation production of saxions. These high f_a/N solutions, however intriguing, are all excluded because such high values of f_a/N suppress the saxion and $\widetilde{Z}_1$ lifetimes, so their decays will affect BBN.

The upshot of Fig. 12 is that, for f_a/N slightly below 10^{13} GeV, the value of T_R has increased to over 10^{11} GeV while maintaining $\Omega_{a\tilde{a}}h^2 = 0.1123$, thus reconciling thermal leptogenesis with the gravitino problem in the AY scenario.

3.3 Scan over PQMSSM parameters including dilution due to entropy injection from saxion decay

While Fig. 12 holds for particular values of the PQMSSM parameters, save for f_a/N, we will now scan over the remaining PQ parameters $m_{\tilde{a}}$ and θ_i, as well as f_a/N, as in Section 2.5. This time, we will adopt $m_s = m_0 = 1$ TeV and $s_i/(f_a/N) = 1$, and allow for saxion-induced entropy dilution of mixed axion/axino DM according to the procedure described in the last section. The results for $\Omega_{\widetilde{Z}_1}h^2 = 0.04$ and $m_{\widetilde{Z}_1} = 430$ GeV are shown in Fig. 13, where we plot the value of T_R needed to maintain $\Omega_{a\tilde{a}}h^2 = 0.1123$ versus PQ breaking scale f_a/N. The line where $r = S_f/S_i = 1$ is shown in magenta. The red points violate BBN bounds due to late decaying $\widetilde{Z}_1$, while the green points violate BBN bounds due to late-time saxion decays ($T_s < 10$ MeV). The light blue points have $> 20\%$ WDM or $> 1\%$ HDM, while the dark blue points satisfy all constraints. The WDM/CDM bound following Boyarsky [37] is again indicated as a dashed blue line. We see now that by including dilution of DM from saxion production and decay, the allowed points now reach to $T_R \sim 10^9 - 10^{12}$ GeV for $f_a/N \sim 5 \times 10^{11} - 15 \times 10^{12}$ GeV. These points evidently reconcile thermal leptogenesis with the gravitino problem, and allow for somewhat higher T_R values than those generated in Fig. 3, where entropy injection was neglected.

In Fig. 14, we plot the axion mis-alignment angle θ_i. Unlike the previous results in Fig. 4 with no entropy injection, the allowed values of θ_i with $T_R > 2 \times 10^9$ GeV span a range from 0 to ~ 1.8 radians: for higher values of T_R, larger values of θ_i can be tolerated since the relic abundance of axions is now diluted by saxion decay.

To see whether axinos or axions dominate the DM density including entropy from saxions, in Fig. 15 we plot the same points, but this time versus axion relic density $\Omega_a h^2$. We see that the bulk of points with $T_R > 2 \times 10^9$ GeV that are BBN-allowed indeed have *mainly axion* CDM. Note that the point shown in Fig. 12, which has $\theta_i = 0.05$ and mainly axino DM (at $T_R > 2 \times 10^9$ GeV), corresponds to the few points of Fig. 15 at low $\Omega_a h^2$ and

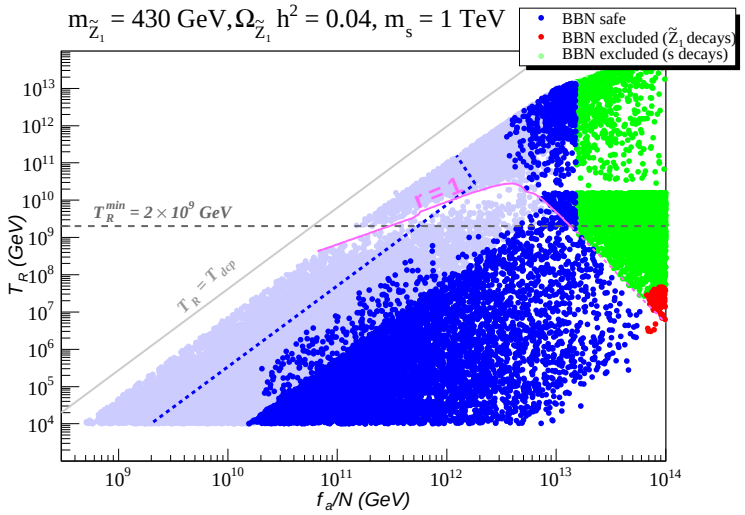

Figure 13: Allowed and disallowed points in the f_a *vs.* T_R plane for $\Omega_{\widetilde{Z}_1}h^2 = 0.04$ and $m_{\widetilde{Z}_1} = 430$ GeV, with $m_s = 1$ TeV.

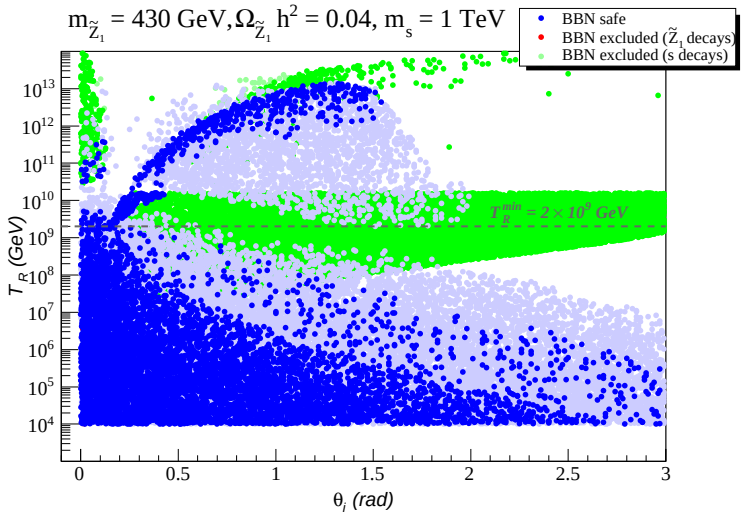

Figure 14: Allowed and disallowed points in the θ_i *vs.* T_R plane for $\Omega_{\widetilde{Z}_1}h^2 = 0.04$ and $m_{\widetilde{Z}_1} = 430$ GeV, with $m_s = 1$ TeV.

is not the most common scenario, since it requires quite small values of the mis-alignment angle. Given that $f_a/N \sim 3 - 15 \times 10^{12}$ GeV, we expect the axion mass $m_a \sim 0.4 - 2$ μeV, somewhat below the range where ADMX is searching [48].

3.4 More general scan over MSSM parameters

Next, we generalize our results for a general PQMSSM model, where we now allow $\Omega_{\widetilde{Z}_1}$ and $m_{\widetilde{Z}_1}$ to be free parameters included in our scan, as in Fig. 6. For simplicity we keep the saxion mass fixed at $m_s = 1$ TeV. The result is shown in Fig. 16, where the red (green) points are excluded due to the BBN constraints on $\widetilde{Z}_1$ (saxion) decays. Two important conclusions can be drawn when Figs. 6 and 16 are compared. First, due to the saxion

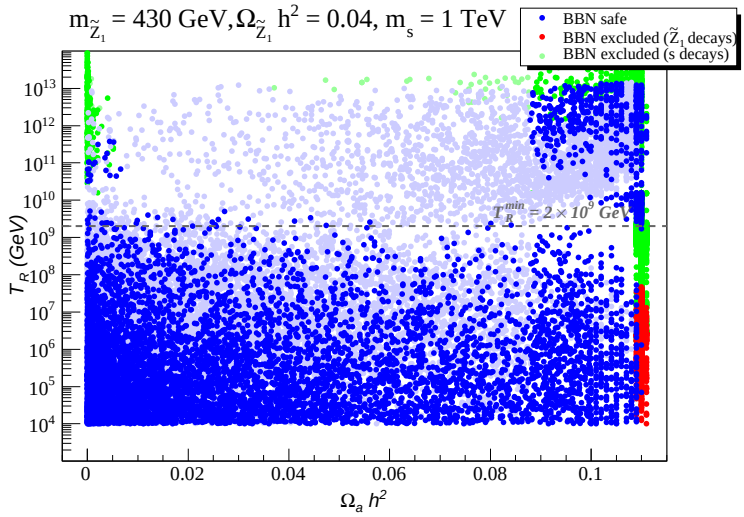

Figure 15: Allowed and disallowed points in the $\Omega_a h^2$ *vs.* T_R plane for $\Omega_{\widetilde{Z}_1} h^2 = 0.04$ and $m_{\widetilde{Z}_1} =$ 430 GeV, with $m_s = 1$ TeV.

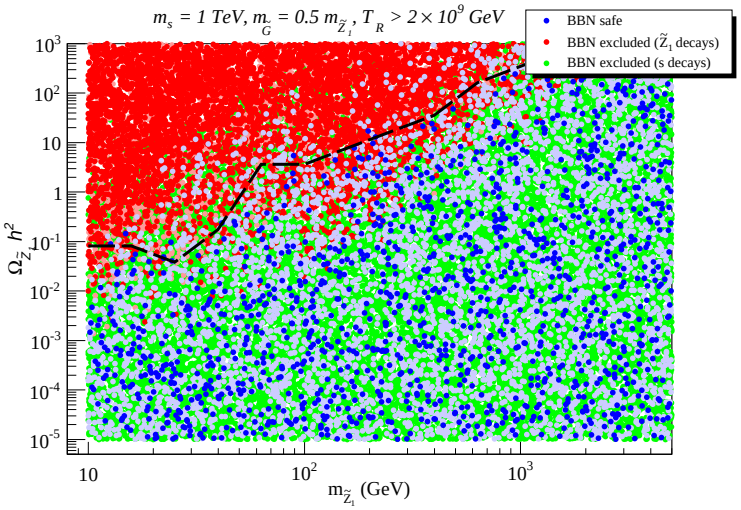

Figure 16: Allowed and disallowed points in the $\Omega_{\widetilde{Z}_1} h^2$ *vs.*$m_{\widetilde{Z}_1}$ plane for a general scan over SUSY models with a bino $\widetilde{Z}_1$ and $m_s = 1$ TeV. For all points, we require $T_R > 2 \times 10^9$ GeV. In this plot, we include the effect of entropy production from saxion decay. Dark blue points are consistent with BBN and have mainly CDM with at most 20% WDM and/or 1% HDM admixture. The region below the dashed line represents the MSSM parameter space where 99% of the DM/BBN consistent solutions lie when applying weaker WDM/HDM requirements as discussed in the text.

dilution of the neutralino relic density, the BBN bounds on $\Omega_{\widetilde{Z}_1}$ are less severe and a larger portion of the MSSM parameter space can be consistent with thermal leptogenesis. On the other hand, the PQ parameter space becomes more constrained due to the BBN bounds on saxion decays, which are shown as green points in Fig. 16. As a consequence, the density of CDM/BBN consistent solutions with $T_R > 2 \times 10^9$ GeV (dark blue dots) is clearly smaller than in Fig. 6.

3.5 Thermal leptogenesis-allowed regions of the mSUGRA plane

As a last point of this study, let us apply our general results to the showcase mSUGRA model in the m_0 *vs.* $m_{1/2}$ plane. In order to make our results independent of a particular choice of PQ parameters, we consider the bounds on $\Omega_{\widetilde{Z}_1}h^2$ obtained from the general PQMSSM scan in Sections 2.5 and 3.4 (for the case with saxion entropy injection). These bounds are represented by the dashed lines in Figs. 6 and 16. We may then translate this into a contour in the m_0 *vs.* $m_{1/2}$ plane of mSUGRA for $A_0 = 0$, $\mu > 0$ and constant $\tan\beta$, as shown for the cases of $\tan\beta = 10$, 50 and 55 in Fig. 17. The gray regions are excluded because they violate the LEP2 limits on Higgs and sparticle masses[2] or have a stau as next-to-next-to-lightest SUSY particle (NNLSP); these latter cases require special treatment as for example in Ref. [50].

In frame *a)*, we show the mSUGRA m_0 *vs.* $m_{1/2}$ plane for $\tan\beta = 10$. The strips of dark blue and purple points show the regions that allow for $T_R > T_R^{min}$, while maintaining $\Omega_{a\tilde{a}}h^2 = 0.1123$ and respecting bounds from BBN. The subset of purple points at low $m_{1/2}$ satisfies in addition the following constraints on low energy (LE) observables:

1. $\Delta a_\mu^{SUSY} = (7.90 - 37.39) \times 10^{-10}$,
2. $BR(b \to s\gamma) = (2.79 - 4.3) \times 10^{-4}$,
3. $BR(B_s \to \mu^+\mu^-) < 4.7 \times 10^{-8}$,
4. $0.55 < BR(B_u \to \tau^+\nu_\tau)^{\rm MSSM}/BR(B_u \to \tau^+\nu_\tau)^{\rm SM} < 2.71$

where $1.-3.$ were calculated using `Isajet/Isatools` and 4. was calculated using `Superiso`.

We see the AY consistent regions, although broader, are very similiar to the classic mSUGRA regions with neutralino dark matter: the stau co-annihilation region at low m_0 and the light Higgs resonance region where $\widetilde{Z}_1\widetilde{Z}_1 \to h$ at $m_{1/2} \sim 150$ GeV. The reason is that a rather low abundance of thermal neutralinos is required in the AY scenario to satisfy BBN constraints on late decaying $\widetilde{Z}_1$s. For comparison, the classic mSUGRA strips where the neutralino relic density $\Omega_{\widetilde{Z}_1}h^2$ lies within the limits 0.1123 ± 0.0105 are shown as yellow/orange points.

Invoking next the $\Omega_{\widetilde{Z}_1}$ *vs.* $m_{\widetilde{Z}_1}$ contour of Fig. 16, which includes the effect of entropy generation from a $m_s = 1$ TeV saxion, the AY consistent regions broaden out considerably. The region with $T_R > T_R^{min}$ is denoted here by light blue points, and expands to fill the lower m_0 portion of the m_0 *vs.* $m_{1/2}$ plane. The portion of the leptogenesis consistent region including saxion decays and LE constraints is labelled by pink dots, and requires $m_{1/2} \lesssim 550$ GeV, so as to allow for a significant contribution to $(g-2)_\mu$ by light smuons. The remaining unshaded (white) region of the mSUGRA plane does not allow for an AY reconciliation of thermal leptogenesis with the gravitino problem, with or without saxion decays, mainly because the relic density of neutralinos is so large that the BBN constraints on late decaying $\widetilde{Z}_1$ are violated.

[2]The LEP2 limit on a SM-like Higgs scalar h is $m_h > 114.4$ GeV. Here, we use $m_h > 111$ GeV allowing for an approximate 3 GeV error on the theory calculation of m_h. For the SUSY mass limits we use those implemented in `Superiso` [49].

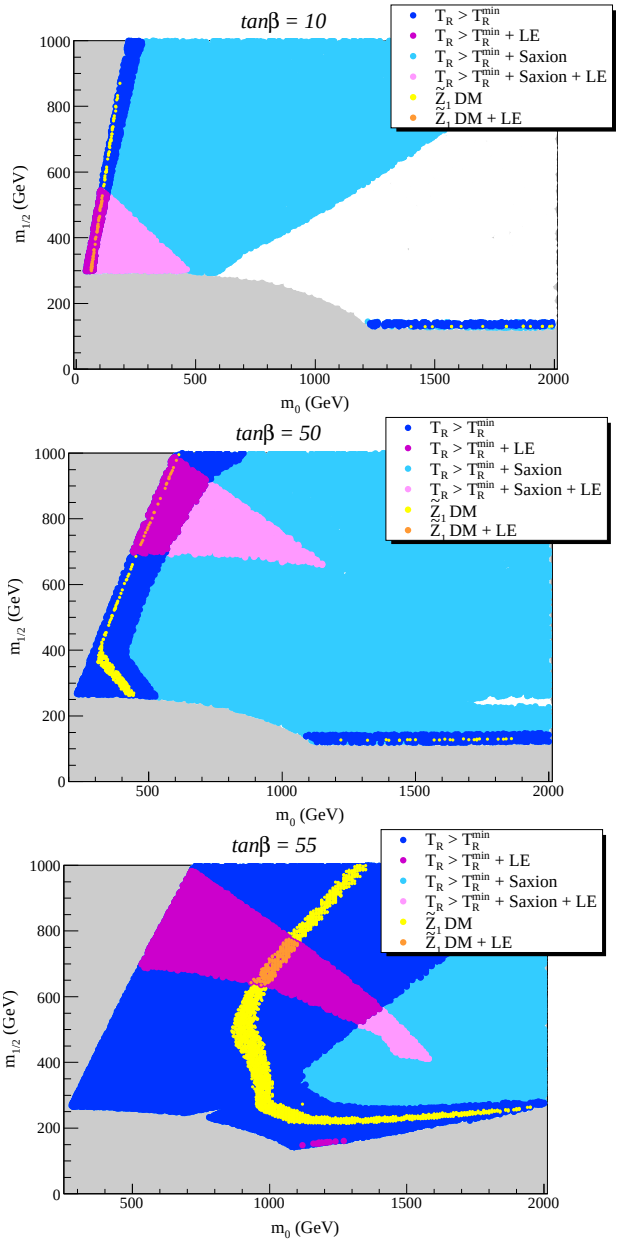

Figure 17: Regions in the m_0 *vs.* $m_{1/2}$ plane of the mSUGRA model with $A_0 = 0$ and $\mu > 0$ which satisfy 1. $T_R > T_R^{min} = 2 \times 10^9$ GeV (dark blue), 2. $T_R > T_R^{min}$ and LE constraints (purple), 3. $T_R > T_R^{min}$ with saxion entropy injection (light blue) and 4. $T_R > T_R^{min}$ with saxion entropy injection and LE constraints (pink). For comparison, the yellow/orange points indicate the classic mSUGRA regions with $\Omega_{\widetilde{Z}_1} h^2 = 0.1123 \pm 0.0105$. We show frames for *a*) $\tan\beta = 10$, *b*) $\tan\beta = 50$ and *c*) $\tan\beta = 55$.

Frame *b*) of Fig. 17, shows the analogous plot for $\tan\beta = 50$. In this case, b- and τ-Yukawa couplings increase greatly, while the value of m_A drops, enabling efficient annihilation of neutralinos via stau coannihilation or s-channel A exchange. The apparent neutralino abundance $\Omega_{\widetilde{Z}_1} h^2$ is severely reduced, and less constrained by BBN. The area of

leptogenesis-consistent regions increases. Furthermore, the SUSY contributions to $b \to s\gamma$ and $(g-2)_\mu$ increase with increasing $\tan\beta$, and so the region which is consistent with LE constraints moves to higher $m_{1/2}$ values. If saxion entropy production is added, only a tiny region at $m_0 > 1700$ GeV with $m_{1/2} \sim 200$ GeV is not allowed by the AY scenario.

Finally, frame *c*) shows the case of $\tan\beta = 55$, where the A-resonance dominates the $\widetilde{Z}_1\widetilde{Z}_1$ annihilation amplitudes. Here, we see that a huge swath of parameter space is AY-consistent, even without the effect of saxion decays. By including entropy from saxion decay, the entire m_0 *vs.* $m_{1/2}$ plane becomes AY-consistent. The part which is consistent with LE constraints follows suit, leading to a large region of parameter space that is consistent with all constraints.

4. Conclusions

In this paper, we reported on investigations of the viability of the Asaka-Yanagida suggestion that a mass hierarchy with $m(\text{sparticle}) > m_{\widetilde{G}} > m_{\tilde{a}}$ can be used to reconcile thermal leptogenesis, which requires $T_R \gtrsim 2\times 10^9$ GeV, with the gravitino problem, which seemingly requires much lower T_R to avoid BBN constraints and overproduction of neutralino dark matter. In the AY scenario, the $\widetilde{G}$ decays inertly to $a\tilde{a}$. BBN constraints on sparticle $\to \widetilde{G}$ + particle can be avoided because the much faster decays sparticle $\to \tilde{a}$ + particle are now allowed. We re-examined the AY scenario in Sec. 2 by including 1. updated measurements on the total dark matter abundance $\Omega_{DM}h^2 \simeq 0.1123$, 2. updated calculations of thermal axino and gravitino production, 3. the contribution of relic axions and 4. BBN constraints on late decaying $\widetilde{Z}_1$s. Furthermore, in Sec. 3, we included dilution of dark matter by saxion production and decay. The latter effect can be neglected if m_s is in the multi-TeV range and the initial saxion field strength s_i is somewhat smaller than the PQ breaking scale f_a/N.

We found in Sec. 2, neglecting the saxion entropy effect, that the AY scenario does work under the conditions that *(i)* f_a/N is rather large $\gtrsim 10^{12}$ GeV, implying a somewhat lighter axion than is presently searched for by ADMX [48], *(ii)* the apparent neutralino relic density $\Omega_{\widetilde{Z}_1}h^2$ is not too big: $\Omega_{\widetilde{Z}_1}h^2 \lesssim 1$, *(iii)* the value of $m_{\widetilde{Z}_1}$ is at least in the several hundred GeV range in order to hasten the $\widetilde{Z}_1$ decay rate, and *(iv)* the axion mis-alignment angle θ_i is on the small side $\lesssim 0.5$ to suppress overproduction of axions when f_a/N is large.

By including saxion production and decay in Sec. 3, we can dilute the axino and also axion DM abundance, which in turn allows for somewhat higher values of $T_R \sim 10^{12}$ GeV to be generated. The saxion mass m_s needs to be rather large to avoid BBN constraints on late decaying saxions if T_R is to be high. In this case, the DM is likely to be *mainly axions*, although a few cases with mainly axino DM were generated. The axion mis-alignment angle need not be small here since the axion abundance can be suppressed by entropy injection from saxions. We have also found that a large portion of the MSSM parameter space ($\Omega_{\widetilde{Z}_1}$ and $m_{\widetilde{Z}_1}$) can be consistent with high T_R and still avoid the BBN bounds on late decaying neutralinos, due to the dilution of the neutralino relic density after the entropy injection from saxion decays.

The observable consequences of our final results are as follows. If the AY scenario with $m(\text{sparticle}) > m_{\widetilde{G}} > m_{\tilde{a}}$ is to reconcile thermal leptogenesis with the gravitino problem, then we expect several broad results to ensue:

1. discovery of SUSY at the LHC, with a reconstructed $\Omega_{\widetilde{Z}_1}h^2$ not too large, lest $\widetilde{Z}_1$s are produced at too large a rate in the early universe, and their late decays disrupt BBN;

2. a SUSY mass spectrum to be consistent with SUGRA models with a rather light (but still weak scale) gravitino, since the gravitino mass must be lighter than all observable sparticles;

3. a mainly bino-like $\widetilde{Z}_1$, to quicken decays into $\tilde{a}\gamma/Z$, with mass $m_{\widetilde{Z}_1}$ in the hundreds of GeV range, which also helps diminish the lifetime;

4. no direct or indirect detection of neutralino (WIMP) dark matter;

5. finally, we expect discovery of an axion to be likely, but in the mass range $\sim 0.1 - 2$ μeV, somewhat below the values presently being explored.

Acknowledgments

This research was supported in part by the U.S. Department of Energy, by the Fulbright Program and CAPES (Brazilian Federal Agency for Post-Graduate Education), and by the French ANR project `ToolsDMColl`, BLAN07-2-194882.

References

[1] For some reviews, see *e.g.* V. Barger, D.Marfatia and K. Whisnant, *Int. J. Mod. Phys.* **E12** (2003) 569; L.Camilleri, E. Lisi and J. Wilkerson, *Ann. Rev. Nucl. Part. Sci.* **58** (2008) 343; B. Kayser, in C. Amsler *et al.* [Particle Data Group], *Phys. Lett.* **B 667** (2008) 1.

[2] M. Gell-Mann, P. Ramond and R. Slansky, in *Supergravity, Proceedings of the Workshop*, Stony Brook, NY 1979 (North-Holland, Amsterdam); T. Yanagida, KEK Report No. 79-18, 1979; R. Mohapatra and G. Senjanovic, *Phys. Rev. Lett.* **44** (1980) 912.

[3] M. Fukugita and T. Yanagida, *Phys. Lett.* **B 174** (1986) 45; M. Luty, *Phys. Rev.* **D 45** (1992) 455; W. Buchmüller and M. Plumacher, *Phys. Lett.* **B 389** (1996) 73 and *Int. J. Mod. Phys.* **A 15** (2000) 5047; R. Barbieri, P. Creminelli, A. Strumia and N. Tetradis, *Nucl. Phys.* **B 575** (2000) 61; G. F. Giudice, A. Notari, M. Raidal, A. Riotto and A. Strumia, *Nucl. Phys.* **B 685** (2004) 89; for a recent review, see W. Buchmüller, R. Peccei and T. Yanagida, *Ann. Rev. Nucl. Part. Sci.* **55** (2005) 311.

[4] V. Kuzmin, V. Rubakov and M. Shaposhnikov, *Phys. Lett.* **B 155** (1985) 36; F. Klinkhammer and N. Manton, *Phys. Rev.* **D 30** (1984) 2212.

[5] W. Buchmüller, P. Di Bari and M. Plumacher, *Nucl. Phys.* **B 643** (2002) 367 and Erratum-ibid,**B793** (2008) 362; *Annals Phys.* **315** (2005) 305 and *New J. Phys.* **6** (2004) 105.

[6] H. Baer and X. Tata, *Weak Scale Supersymmetry: From Superfields to Scattering Events*, (Cambridge University Press, 2006).

[7] S. Weinberg, *Phys. Rev. Lett.* **48** (1982) 1303.

[8] M. Khlopov and A. Linde, *Phys. Lett.* **B 138** (1984) 265.

[9] G. Lazarides and Q. Shafi, *Phys. Lett.* **B 258** (1991) 305; K. Kumekawa, T. Moroi and T. Yanagida, *Prog. Theor. Phys.* **92** (1994) 437; T. Asaka, K. Hamaguchi, M. Kawasaki and T. Yanagida, *Phys. Lett.* **B 464** (1999) 12.

[10] W. Buchmuller, L. Covi, K. Hamaguchi, A. Ibarra and T. Yanagida, *J. High Energy Phys.* **0703** (2007) 037

[11] L. Covi, J. Hasenkamp, S. Pokorski and J. Roberts, *J. High Energy Phys.* **0911** (2009) 003.

[12] H. Baer, S. Kraml, A. Lessa and S. Sekmen, JCAP **1011** (2010) 040.

[13] R. Peccei and H. Quinn, *Phys. Rev. Lett.* **38** (1977) 1440 and *Phys. Rev.* **D 16** (1977) 1791.

[14] S. Weinberg, *Phys. Rev. Lett.* **40** (1978) 223; F. Wilczek, *Phys. Rev. Lett.* **40** (1978) 279.

[15] J. E. Kim, *Phys. Rev. Lett.* **43** (1979) 103; M. A. Shifman, A. Vainstein and V. I. Zakharov, *Nucl. Phys.* **B 166** (1980) 493.

[16] M. Dine, W. Fischler and M. Srednicki, *Phys. Lett.* **B 104** (1981) 199; A. P. Zhitnitskii, *Sov. J. Nucl.* **31** (1980) 260.

[17] H. P. Nilles and S. Raby, *Nucl. Phys.* **B 198** (1982) 102; J. E. Kim, *Phys. Lett.* **B 136** (1984) 378; J. E. Kim and H. P. Nilles, *Phys. Lett.* **B 138** (1984) 150.

[18] For recent reviews of axino dark matter, see F. Steffen, *Eur. Phys. J.* **C 59** (2009) 557; L. Covi and J. E. Kim, *New J. Phys.* **11** (2009) 105003.

[19] A. Cohen, D. Kaplan and A. Nelson, *Phys. Lett.* **B 388** (1996) 588.

[20] H. Baer, S. Kraml, A. Lessa, S. Sekmen and X. Tata, *J. High Energy Phys.* **1010** (2010) 018.

[21] K. Choi, A. Falkowski, H. P. Nilles, M. Olechowski and S. Pokorski, *J. High Energy Phys.* **0411** (2004) 076; K. Choi, A. Falkowski, H. P. Nilles and M. Olechowski, *Nucl. Phys.* **B 718** (2005) 113; K. Choi, K-S. Jeong, *J. High Energy Phys.* **0701** (2007) 103; A. Falkowski, O. Lebedev and Y. Mambrini, *J. High Energy Phys.* **0511** (2005) 034; H. Baer, E. Park, X. Tata and T. T. Wang, *J. High Energy Phys.* **0608** (2006) 041; *Phys. Lett.* **B 641** (2006) 447; *J. High Energy Phys.* **0706** (2007) 033.

[22] T. Asaka and T. Yanagida, *Phys. Lett.* **B 494** (2000) 297.

[23] E. Komatsu *et al.* (WMAP collaboration), arXiv:1001.4538 (2010).

[24] For a recent review, see R. Arnowitt and P. Nath, arXiv:0912.2273 (2009).

[25] K. Rajagopal, M. Turner and F. Wilczek, *Nucl. Phys.* **B 358** (1991) 447.

[26] J. E. Kim, A. Masiero and D. V. Nanopoulos, *Phys. Lett.* **B 139** (1984) 346; L. Covi, J. E. Kim and L. Roszkowski, *Phys. Rev. Lett.* **82** (1999) 4180.

[27] L. Covi, H. B. Kim, J. E. Kim and L. Roszkowski, *J. High Energy Phys.* **0105** (2001) 033.

[28] A. Brandenburg and F. Steffen, JCAP**0408** (2004) 008.

[29] A. Strumia, *J. High Energy Phys.* **1006** (2010) 036.

[30] H. Baer, C. Balazs and A.Belyaev, *J. High Energy Phys.* **0203** (2002) 042.

[31] H. Baer, C. Balazs, A.Belyaev, J. K. Mizukoshi, X. Tata and Y. Wang, *J. High Energy Phys.* **0207** (2002) 050.

[32] F. Paige, S. Protopopescu, H. Baer and X. Tata, `hep-ph/0312045`; http://www.nhn.ou.edu/∼isajet/

[33] M. Bolz, A. Brandenburg and W. Buchmuller, *Nucl. Phys.* **B 606** (2001) 518; J. Pradler and F. Steffen, *Phys. Rev.* **D 75** (2007) 023509; V. S. Rychkov and A. Strumia, *Phys. Rev.* **D 75** (2007) 075011.

[34] L. F. Abbott and P. Sikivie, *Phys. Lett.* **B 120** (1983) 133; J. Preskill, M. Wise and F. Wilczek, *Phys. Lett.* **B 120** (1983) 127; M. Dine and W. Fischler, *Phys. Lett.* **B 120** (1983) 137; M. Turner, *Phys. Rev.* **D 33** (1986) 889; L. Visinelli and P. Gondolo, *Phys. Rev.* **D 80** (2009) 035024.

[35] H. Baer, A. Box and H. Summy, *J. High Energy Phys.* **0908** (2009) 080.

[36] K. Jedamzik, M. LeMoine and G. Moultaka, JCAP**0607** (2006) 010.

[37] M. Viel, G. D. Becker, J. S. Bolton, M. G. Haehnelt, M. Rauch and W. L. W. Sargent, Phys. Rev. Lett. **100** (2008) 041304; A. V. Maccio' and F. Fontanot, arXiv:0910.2460 [astro-ph.CO]; A. Boyarsky, J. Lesgourgues, O. Ruchayskiy and M. Viel, JCAP **0905** (2009) 012; D. Boyanovsky and J. Wu, arXiv:1008.0992 [astro-ph.CO].

[38] S. Hannestad, A. Mirizzi, G. G. Raffelt and Y. Y. Y. Wong, JCAP **1008** (2010) 001.

[39] R. H. Cyburt, J. Ellis, B. D. Fields and K. A. Olive, *Phys. Rev.* **D 67** (2003) 103521; R. H. Cyburt, J. Ellis, B. D. Fields, F. Luo, K. Olive and V. Spanos, JCAP**0910** (2009) 021.

[40] M. Kawasaki, K. Kohri and T. Moroi, *Phys. Lett.* **B 625** (2005) 7 and *Phys. Rev.* **D 71** (2005) 083502; K. Kohri, T. Moroi and A. Yotsuyanagi, *Phys. Rev.* **D 73** (2006) 123511; for an update, see M. Kawasaki, K. Kohri, T. Moroi and A. Yotsuyanagi, *Phys. Rev.* **D 78** (2008) 065011.

[41] K. Jedamzik, *Phys. Rev.* **D 70** (2004) 063524 and *Phys. Rev.* **D 74** (2006) 103509.

[42] J. Ellis, T. Falk and K. Olive, *Phys. Lett.* **B 444** (1998) 367; J. Ellis, T. Falk, K. Olive and M. Srednicki, *Astropart. Phys.* **13** (2000) 181; M.E. Gómez, G. Lazarides and C. Pallis, *Phys. Rev.* **D 61** (2000) 123512 and *Phys. Lett.* **B 487** (2000) 313; A. Lahanas, D. V. Nanopoulos and V. Spanos, *Phys. Rev.* **D 62** (2000) 023515; R. Arnowitt, B. Dutta and Y. Santoso, *Nucl. Phys.* **B 606** (2001) 59; see also Ref. [30].

[43] M. Drees and M. Nojiri, *Phys. Rev.* **D 47** (1993) 376; H. Baer and M. Brhlik, *Phys. Rev.* **D 57** (1998) 567; H. Baer, M. Brhlik, M. Diaz, J. Ferrandis, P. Mercadante, P. Quintana and X. Tata, *Phys. Rev.* **D 63** (2001) 015007; J. Ellis, T. Falk, G. Ganis, K. Olive and M. Srednicki, *Phys. Lett.* **B 510** (2001) 236; L. Roszkowski, R. Ruiz de Austri and T. Nihei, *J. High Energy Phys.* **0108** (2001) 024; A. Djouadi, M. Drees and J. L. Kneur, *J. High Energy Phys.* **0108** (2001) 055; A. Lahanas and V. Spanos, *Eur. Phys. J.* **C 23** (2002) 185.

[44] K. L. Chan, U. Chattopadhyay and P. Nath, *Phys. Rev.* **D 58** (1998) 096004; J. Feng, K. Matchev and T. Moroi, *Phys. Rev. Lett.* **84** (2000) 2322 and *Phys. Rev.* **D 61** (2000) 075005; see also H. Baer, C. H. Chen, F. Paige and X. Tata, *Phys. Rev.* **D 52** (1995) 2746 and *Phys. Rev.* **D 53** (1996) 6241; H. Baer, C. H. Chen, M. Drees, F. Paige and X. Tata, *Phys. Rev.* **D 59** (1999) 055014; for a model-independent approach, see H. Baer, T. Krupovnickas, S. Profumo and P. Ullio, *J. High Energy Phys.* **0510** (2005) 020.

[45] M. Kawasaki, K. Nakayama and M. Senami, JCAP**0803** (2008) 009.

[46] J. E. Kim, *Phys. Rev. Lett.* **67** (1991) 3465.

[47] R. Scherrer and M. S. Turner, *Phys. Rev.* **D 31** (1985) 681; see also G. Lazarides, R. Schaefer, D. Seckel and Q. Shafi, *Nucl. Phys.* **B 346** (1990) 193 and J. E. Kim, Ref. [46]; see also J. Hasenkamp and J. Kersten, arXiv:1008.1740 [hep-ph].

[48] L. Duffy *et al.*, *Phys. Rev. Lett.* **95** (2005) 091304 and *Phys. Rev.* **D 74** (2006) 012006; for a review, see S. Asztalos, L. Rosenberg, K. van Bibber, P. Sikivie and K. Zioutas, *Ann. Rev. Nucl. Part. Sci.* **56** (2006) 293.

[49] F. Mahmoudi, *Comput. Phys. Commun.* **178** (2008) 745

[50] A. Freitas, F. Steffen, N. Tajuddin and D. Wyler, *Phys. Lett.* **B 679** (2009) 270 and *Phys. Lett.* **B 682** (2009) 193.

[51] K. Nakamura *et al.* (Particle Data Group), *J. Phys. G***37** (2010) 075021.